Scientia Iranica B (2013) 20 (1), 141–151

Sharif University of Technology

Scientia Iranica

Transactions B: Mechanical Engineering

www.sciencedirect.com

Evaluation of simultaneous effects of inlet stagnation pressure and heat transfer on condensing water-vapor flow in a supersonic Laval nozzle

E. Amiri Rad [a,*], M.R. Mahpeykar [b,1], A.R. Teymourtash [b,1]

[a] *Department of Mechanical Engineering, Hakim Sabzevari University, Sabzevar, P.O. Box: 9617976487, Iran*

[b] *Department of Mechanical Engineering, Ferdowsi University of Mashhad, Mashhad, P.O. Box: 91775-1111, Iran*

Received 15 October 2011; revised 14 March 2012; accepted 24 October 2012

KEYWORDS

Condensation flow;
Inlet stagnation pressure;
Laval nozzle;
Nucleation;
Supercooled steam;
Volumetric heat transfer.

Abstract In supersonic two-phase flows of steam, under the influence of rapid expansion, the vapor becomes supersaturated. Following this condition, nucleation happens during the vapor phase; formed tiny droplets grow along the passage and, therefore, the condensation phenomenon occurs. The effects of the condensation phenomenon in power steam turbines include efficiency drop and mechanical damage. In the previous work of the authors, volumetric heating was introduced as an approach towards reducing the mentioned damage and loss. However, further investigations revealed that heating decreases the mass flow rate, which can be increased by adjusting the inlet stagnation pressure. In this paper, using a semi-analytical and a one-dimensional modeling approach, the simultaneous effects of volumetric heat transfer and inlet stagnation pressure variation are investigated in order to remedy the mass flow rate reduction. The results show that increasing the inlet stagnation pressure up to 5% can fix the mass flow rate of the non-adiabatic flow, compared to the adiabatic flow under the same conditions.

1. Introduction

Steam turbines provide a significant percentage of global electrical power. One of the main problems related to this equipment is the condensation of vapor and engendering of wet flow in low pressure stages.

This process creates a great amount of mechanical and thermodynamic loss and, therefore, engineers take, roughly, a one percent decrease in turbine efficiency for each percent of wetness fraction. Considering the amount of power produced by this method, it is a huge loss on a global scale.

When steam expands from an initially superheated or saturated state, it cools. Sometimes its temperature becomes lower than the local saturation value and the fluid becomes supersaturated. To revert to the equilibrium state, there is no way except the formation of droplets and this leads the flow to become two-phase.

Wet steam is usually considered as a two-phase flow, where the droplets are carried by bulk vapor. The first step in droplet formation is the nucleation stage, and considering the purity of water, the nucleation mechanism is homogenous. Various one-, two- or three-dimensional analyses of this type of flow can be found in the literature (e.g. [1–5]).

In most previously presented research, the flow is considered adiabatic. In this research and in continuation of the previous work of these authors [6], the flow is considered to be non-adiabatic. Regarding this description, a semi-analytical, Eulerian–Lagrangian model is applied to study the mentioned flow.

In this paper, initially, the mathematical model is explained. Then, different nucleation rate expressions are studied and the most suitable one is selected. Finally, the effects of simultaneous volumetric heat transfer and inlet stagnation pressure variations are investigated.

* Corresponding author. Tel.: +98 5714410104.
E-mail addresses: Ehsan_amech@yahoo.com (E. Amiri Rad), mahpeymr@um.ac.ir (M.R. Mahpeykar), teymourtash@um.ac.ir (A.R. Teymourtash).
[1] Tel.: +98 511 8806000.

Peer review under responsibility of Sharif University of Technology.

Production and hosting by Elsevier

1026-3098 © 2013 Sharif University of Technology. Production and hosting by Elsevier B.V. All rights reserved.
doi:10.1016/j.scient.2012.12.009

Nomenclature

A	area
C_p	specific heat at constant pressure
D_e	equivalent diameter
f	friction factor
ΔG	change in Gibbs free energy
Qc	integration of volumetric heat transfer on surface area
M	total mass flow rate
x	distance along duct axis
L	Nozzle throat length
X, Y	functions of temperature and density in equation of state
J	rate of formation of critical droplets per unit volume and time
Kn	Knudsen number
L	latent heat
Ma	mach number
m_r	mass of droplet
P	vapor pressure
P_{0in}	inlet total pressure
$P_s(T_G)$	saturation pressure at T_G
q	condensation coefficient
R	gas constant for water vapor
r	radius of droplet
$S\&T$	entropy & temperature
$T_s(P)$	saturation temperature at P
ΔT	degree of supercooling $[T_s(P) - T_G]$
t	time
α_r	coefficient of heat transfer
γ	isentropic component
μ_G	dynamic viscosity of vapor
ρ	density of mixture
λ	coefficient of thermal conductivity
σ	surface tension
$\rho_s(T_L, r)$	density corresponding to saturation pressure at temperature T_L over a surface of curvature r
Sc	Schmidt number

Subscripts

G	vapor phase
L	liquid phase
0	stagnation condition
S	saturation

Superscript

U	velocity
$\dot{q}$	volumetric heat transfer rate
Q	total heat transfer rate
$*$	critical condition

2. Model description

In this mathematical model, wet steam flow is modeled using a semi-analytical, rather than fully numerical, technique. The gas dynamic flow equations are derived assuming both steady and one-dimensional flow. The flow is considered as a whole and, at each point in the nozzle, the formation of new particles is determined by a homogeneous nucleation rate, while the growth of existing droplets is determined by droplet growth equations. Also, in order to apply the volumetric heat transfer, a heat source is used in the convergent section where the steam is only in the vapor phase or dry.

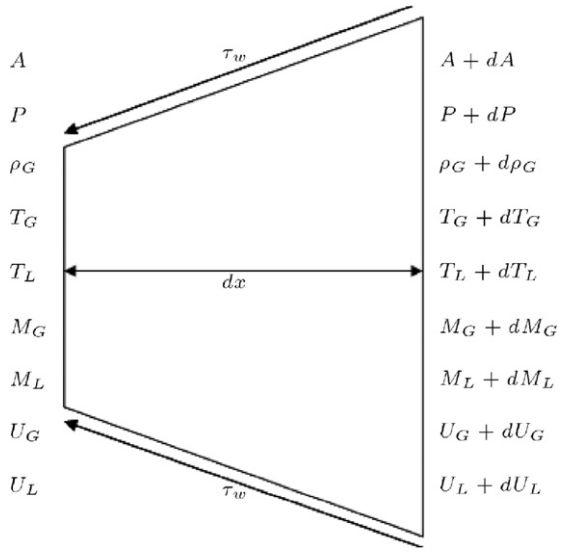

Figure 1: Fluid control volume.

Since the solution is one-dimensional, the surface integral of heat source intensity ($Qc = \dot{q}A$) with the unit (J/mm s) is used for evaluation of heating rate to dry flow in the convergent section.

This model is basically a mixed Eulerian–Lagrangian model, i.e. gas dynamic equations are solved in an Eulerian coordinate, while nucleation and droplet growth equations are performed in a Lagrangian frame. To combine these two methods, the flow path is divided into a large number of small steps and, for each step, the model solves the gas dynamic Eulerian equations. The code determines all flow variables, such as the density, ρ, velocity, u, pressure, p, and temperature, T, while simultaneously tracking the droplet size distribution and the wetness fraction, w, by solving Lagrangian equations of droplet growth.

The only connection between the Lagrangian and Eulerian solutions is via the pressure and temperature fields. At each step, an estimation of the pressure and temperature field is generated by solving the gas dynamics flow equations. This field is then passed to nucleation and droplet growth equations, which compute the wetness distribution on the data. The updated wetness and subcooling fields are then returned to the gas dynamics flow solver for the next stage of the iteration procedure.

Considering a one-dimensional control volume with length dx (Figure 1), neglecting the interphase velocity slip and assuming that the occupied volume by the liquid phase is negligible compared to the volume of the gas phase [6,7], the basic governing equations of gas dynamics are written as follows.

2.1. Conservation of mass

The mass balance equation along the axial of a one-dimensional control volume is presented as:

$$M_L + M_G = Const, \tag{1}$$

where M is mass flow rate and subscripts, L and G, refer to liquid and gas phases, respectively.

Differentiating the above equation and performing a few mathematical operations, the computational form of the mass conservation law for one-dimensional condensing flow is obtained as:

$$\frac{d\rho_G}{\rho_G} + \frac{dA}{A} + \frac{dU_G}{U_G} + \frac{dM_L}{M_G} = 0. \tag{2}$$

2.2. Second Newton's law

By applying the momentum balance law on the mentioned control volume and performing some mathematical work, the differential form of Newton's second law becomes:

$$\frac{dP}{P} + \frac{f\rho_G U_G^2}{2PD_e}dx + \frac{(M_G)\,U_G}{AP}\frac{dU_G}{U_G} + \frac{M_L U_L}{AP}\frac{dU_L}{U_L} = 0. \tag{3}$$

Neglecting interphase slipping, Eq. (3) becomes:

$$\frac{dP}{P} + \frac{f\rho_G U_G^2}{2PD_e}dx + \frac{(M_G + M_L)\,U_G}{AP}\frac{dU_G}{U_G} = 0, \tag{4}$$

where U, D_e, f and A are the velocity, hydraulic diameter, friction factor and area of the channel, respectively.

2.3. First law of thermodynamics

By using the energy balance equation on the mentioned control volume and considering a heat source, the following equation is concluded:

$$d\left[(M - M_L)\left(h_G + \frac{U_G^2}{2}\right) + M_L\left(h_L + \frac{U_L^2}{2}\right)\right] + d\dot{Q} = 0. \tag{5}$$

Neglecting interphase slipping, it can be rewritten as:

$$\frac{dh_G}{C_P T_G} - \frac{d\,(M_L L_h)}{(M_L + M_G)\,C_P T_G} + \frac{U_G^2}{C_P T_G}\frac{dU_G}{U_G} + \frac{d\dot{Q}}{(M_L + M_G)\,C_P T_G} = 0, \tag{6}$$

where, L_h is the latent heat of steam vapor and $d\dot{Q}$ is calculated as:

$$d\dot{Q} = \dot{q}Adx, \tag{7}$$

where, in this equation, $\dot{q}$ is heat power per cubic meter.

For the vapor phase, the enthalpy variation can be calculated as:

$$dh_G = C_p dT_G + \left[U_G - T_G\left(\frac{\partial U_G}{\partial T_G}\right)_P\right]dP. \tag{8}$$

By combining Eqs. (6)–(8), and the state equation that is explained in the next section, the following computational expression is derived for the first law of thermodynamics:

$$\frac{dT_G}{T_G} + \frac{P}{\rho_G C_P T_G}\left(1 - \frac{Y}{X}\right)\frac{dP}{P} + \frac{U_G^2}{C_P T_G}\frac{dU_G}{U_G} + \frac{d\dot{Q}}{(M_L + M_G)\,C_P T_G} = \frac{L_h}{C_P T_G}\frac{dM_L}{(M_L + M_G)}. \tag{9}$$

2.4. Vapor state equation

To improve the accuracy of the solution, the viral state equation with 3 coefficients, suggested by Vukalovic [8], is used as follows:

$$\frac{P}{\rho_G R T_G} = 1 + B_1\rho_G + B_2\rho_G^2 + B_3\rho_G^3, \tag{10}$$

where B_1, B_2 and B_3 are the viral density coefficients which depend on vapor temperature [8]. Differentiating Eq. (10) yields:

$$\frac{dP}{P} - X\frac{d\rho_G}{\rho_G} - Y\frac{dT_G}{T_G} = 0, \tag{11}$$

where X and Y are defined as:

$$X = \frac{\rho_G}{P}\left(\frac{\partial P}{\partial \rho_G}\right)_{T_G} = \frac{1 + 2B_1\rho_G^2 + 3B_2\rho_G^2 + 4B_3\rho_G^3}{1 + B_1\rho_G^1 + B_2\rho_G^2 + B_3\rho_G^3}, \tag{12}$$

$$Y = \frac{T_G}{P}\left(\frac{\partial P}{\partial \rho_G}\right)_{\rho_G} = 1 + \frac{\rho_G T_G}{1 + B_1\rho_G^1 + B_2\rho_G^2 + B_3\rho_G^3} \times \left[\frac{dB_1}{dT_G} + \rho_G\frac{dB_2}{dT_G} + \rho_G^2\frac{dB_3}{dT_G}\right]. \tag{13}$$

2.5. Mach number

The Mach number has a key role in supersonic flow and is defined as:

$$Z = Ma^2 = \left(\frac{U_G}{C}\right)^2, \tag{14}$$

where C is the frozen speed of sound for ideal gas. Differentiating the above equation gives:

$$\frac{dZ}{Z} = 2\frac{dU_G}{U_G} + \frac{d\rho_G}{\rho_G} - \frac{dP}{P}. \tag{15}$$

Using the previous set of Eqs. (2), (4), (9), (11) and (15), the gas dynamics of the flow consist of velocity, pressure, temperature and density fields, which are calculated in an Eulerian framework. But, solution of these equations needs wetness parameters that can be obtained in a Lagrangian framework, as explained in the following section.

2.6. Nucleation rate

Regarding the purity of vapor, the nucleation mechanism is homogeneous. This model of nucleation occurs when the molecules of vapor join together and create a droplet with critical radius and develop an interface at the boundaries of a new phase.

The driving force of nucleation is supersaturation, which is caused when the vapor temperature becomes lower than the saturated value. In this case, the flow becomes unstable and, to retrieve its stability, droplets are created. This process adjusts the free energy and stabilizes the flow.

The required free energy for the formation of a spherical droplet can be obtained as:

$$\Delta G = \Delta G_v + \Delta G_s = -m_r RTLn\left(\frac{P}{P_s\,(T_G)}\right) + 4\pi r^2\sigma_r, \tag{16}$$

where ΔG_v indicates the required energy for creating a droplet bulk and ΔG_s indicates the free energy of the creation surface. In this equation, ΔG_s is always a positive parameter and increases proportionally with r^2, but ΔG_v is always a negative parameter and its amount decreases proportionally with r^3. Therefore, in order to determine the variation patterns of total change

in Gibbs free energy, Eq. (16) is differentiated. Based on this differentiation, it is concluded that a maximum value of Gibbs free energy is obtained when the radius has a critical value. For radii greater than the critical radius, the total amount of Gibbs free energy is increased by an increase in the radius, which means that after this radius, there is spontaneous condensation of vapor. On the other hand, the droplets smaller than the critical droplet evaporate. The critical radius is calculated by the following equation:

$$r^* = \frac{2\sigma_r}{\rho_L R T_G \ln\left[\frac{P}{P_s(T_G)}\right]}. \tag{17}$$

Substituting the critical radius in Eq. (16), the variation of Gibbs free energy for creating critical droplets can be obtained as:

$$\Delta G^* = \frac{16\pi\sigma_r^3}{\rho_L R T_G \ln\left[p/p_s(T_G)\right]}. \tag{18}$$

Figure 2 shows variations of the total Gibbs free energy and their components.

Various theoretical expressions for calculating homogeneous nucleation rates exist in the literature [9–13]. The first theoretical treatment of homogeneous nucleation that is still widely used today is the classical nucleation equation as follows:

$$J_{BD} = q_c \frac{\rho_G^2}{\rho_L}\sqrt{\left(\frac{2\sigma_r}{\pi m}\right)} \exp\left[-\frac{\Delta G^*}{KT_G}\right]. \tag{19}$$

Several refinements of the classical nucleation rate, including Kantrowitz and Courtney expressions [9,10], is presented as:

$$J_{Ka-Co} = \frac{\rho_s(T_G)}{\rho_G \times (1+\phi)} J_{st}, \tag{20}$$

where:

$$\phi = \frac{q_c \rho_G}{\alpha_r}\left(\frac{RT_G}{2\pi}\right)^{0.5}\left(\frac{L_h^2}{RT_G^2} - \frac{L_h}{2T_G}\right), \tag{21}$$

where α_r is the heat transfer coefficient.

Wölk et al. [11] developed an empirical correction function to bring the predictions of classical nucleation theory into quantitative agreement with their nucleation rate measurements. They presented the following expression for the water vapor nucleation rate:

$$J_{H_2O} = J_{BD} \exp\left(-27.56 + \frac{6.5 * 10^3}{T}\right). \tag{22}$$

Finally, Hale [12,13] developed a nucleation model based on scaling arguments which has a temperature dependence that matches the experimental results quite closely:

$$J_{HALE} = J_0 \exp\left(-\frac{W}{kT}\right), \tag{23}$$

where:

$$J_0 = 10^{26}\ \mathrm{cm}^{-3}\ \mathrm{s}^{-1},$$

$$W = \frac{16\pi}{3}\Omega^3 \frac{\left(\frac{T_c}{T} - 1\right)^3}{\left(\ln\left[\frac{P}{P_s(T_G)}\right]\right)^2}, \tag{24}$$

where W is the work of formation of a critical cluster, and Ω is the dimensionless surface entropy per molecule. The value of Ω can be derived from experimental nucleation rate data or estimated from the physical properties of the substance of interest; for the H_2O isotope of water, it is estimated as 1.44, given in [14].

The results of the three presented nucleation equations are compared in Figure 3 for an inlet stagnation pressure of $P_{0in} = 142.4$ kPa and temperature of $T_{0in} = 404$ K. In Figure 4, the pressure ratios obtained for the different models are compared with experimental data presented in [15].

It is clear that Hall's model provides a slightly better fit to the experimental data than the other models. Also, this model is easier to evaluate and is independent of physical parameter correlations. Thus, the model of Hall is used for the nucleation rate expression in this research.

2.7. Droplet growth equations

Droplets that emerge from the nucleation process as supercritical stable droplets will further grow by condensation of the bulk supercooled vapor on their surface. As the vapor molecules condense on the droplet's surface, they give their latent heat to the droplet and, subsequently, there is heat transfer between the droplet and bulk vapor.

Figure 5 shows the temperature variations between a droplet and its surrounding environment [16]. The rate of condensation on a droplet is governed by the rate at which latent heat, L_h, can be carried away from the surface into the bulk supercooled vapor. The relative velocity between the droplet and vapor is neglected here and the droplet is assumed to be spherical and surrounded by an infinite vapor space.

Applying the first law of thermodynamics to a liquid droplet yields:

$$L_h \frac{dm_r}{dt} - 4\pi r^2 \alpha_r (T_L - T_G) = m_r C_L \frac{dT_L}{dt}, \tag{25}$$

where T_L is the droplet temperature, C_L is the specific heat of the liquid phase, m_r is the droplet mass and α_r is the heat transfer coefficient between the droplet and bulk vapor.

Regarding the two layer model described in [16], α_r can be expressed as:

$$\alpha_r = \frac{\lambda}{r\left[1/(1+2\beta K_n) + 3.78K_n/\mathrm{Pr}\right]}; \quad \beta = 0.75,$$
$$\mathrm{Pr} = \frac{C_P \mu_G}{\lambda}, \tag{26}$$

where λ is the heat conduction coefficient of the vapor phase.

Latent heat, heat conduction coefficient, dynamic viscosity and surface tension are functions of temperature.

The heat transfer is driven by a temperature difference between droplet and vapor, $(T_L - T_G)$. The temperature of the droplet depends also on its radius. When the sizes are close to critical size, the temperature of the droplet reaches the saturated temperature of the gas phase. For the large size of droplet, the temperature, T_L, reaches the vapor temperature. Therefore, the droplet temperature can be approximated as [15]:

$$T_L = T_s(P) - \{T_s(P) - T_G\}\frac{r^*}{r}. \tag{27}$$

Using Eqs. (25) and (27), the radius and temperature of the droplet can be calculated in a Lagrangian framework. Also, the total specific entropy of the flow can be calculated from:

$$S = M_G s_G + M_L s_L + S_s, \tag{28}$$

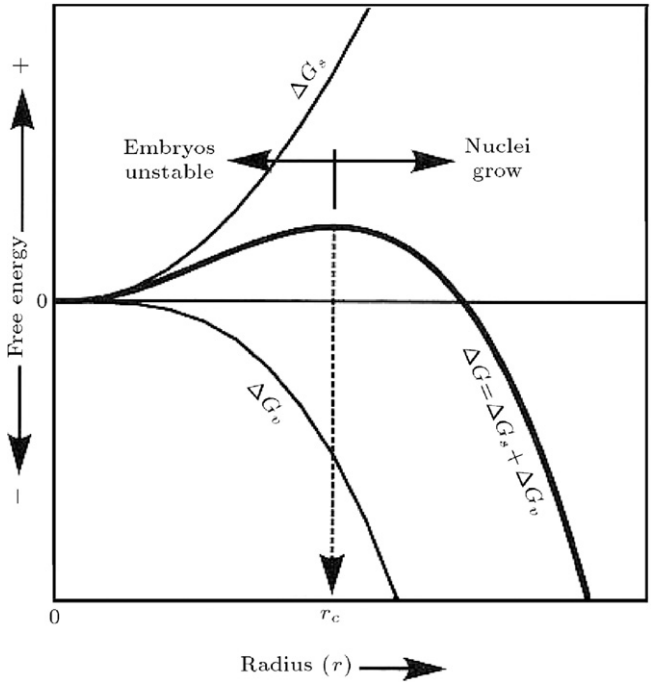

Figure 2: Gibbs free energy variations for droplet creation.

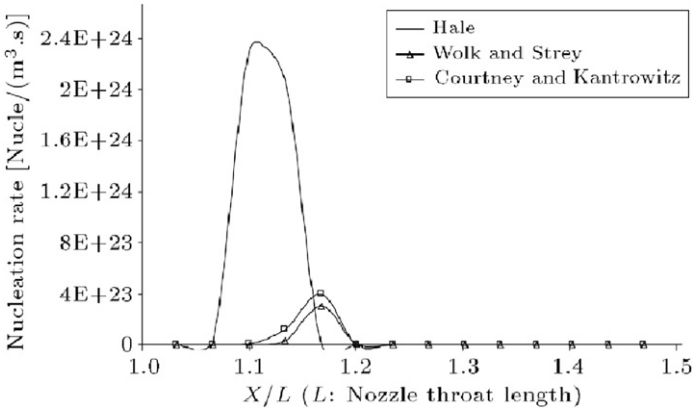

Figure 3: Variation of nucleation rate in the divergent section.

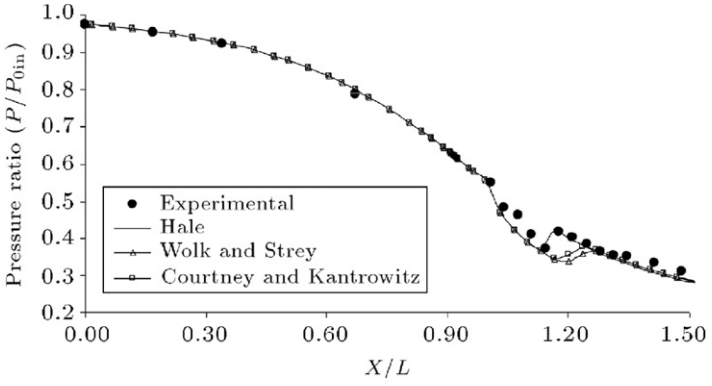

Figure 4: Variation of pressure ratio along the nozzle for different nucleation models.

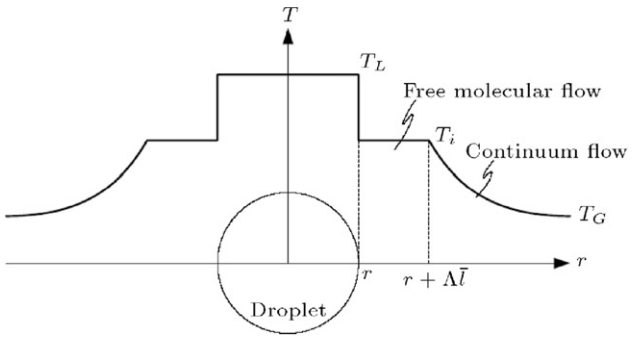

Figure 5: Temperature distribution in the two layer model [16].

where S_s is the entropy of a water droplet surface, s_L is the specific entropy of the liquid phase and s_G is the specific entropy of the vapor phase. s_G can be calculated from [6]:

$$s_G = R\left[(-B_1\rho) + \left(-\rho\frac{dB_1}{dT}\right)\right] + s_0, \tag{29}$$

where s_0 can be obtained from the following equation [6]:

$$s_0 = 0.30773 - 0.46153Ln(\rho) + 1.1095Ln(T) + 7.11756 * 10^{-4}T - \frac{3495}{T^2}. \tag{30}$$

Based on classic thermodynamics, the specific entropy of a water droplet at temperature T_L can be approximated by:

$$s_L = C_L Ln\left(\frac{T_L}{T_D}\right) \tag{31}$$

where C_L is the water specific temperature and T_D is the reference temperature at 273.15 K.

Also, the specific entropy of droplet surfaces is obtained from [17]:

$$S_s = -A_D\left(\frac{\partial\sigma}{\partial T}\right)_P, \tag{32}$$

where A_D and σ denote the droplet surface and surface tension, respectively.

3. Results and discussion

As mentioned previously, $Qc = \dot{q}A\left(\frac{\text{J}}{\text{mm s}}\right)$ is introduced to calculate the amount of heating per length in the convergent section. The results for the heating case and also the inlet stagnation pressure effect are presented in Part I of the results. The case of keeping the mass flow rate constant is given in Part II.

It should be mentioned that in all cases, the stagnation inlet temperature is fixed on $T_{0in} = 404$ K. The horizontal axis in all diagrams is the ratio of axial distance from the nozzle inlet to nozzle throat length.

3.1. Part I

In the first part, volumetric heating was applied to the flow with $P_{0in} = 142.4$ kPa. In order to compensate for the mass flow rate reduction, the inlet stagnation pressure was increased. As the results given in Table 1 indicate, heating the flow causes a reduction of about 2.85% in comparison with the mass flow rate of the adiabatic flow. However, by increasing the inlet stagnation pressure to 2.74%, the reduction in mass flow rate can be compensated.

Table 1: Effects of heating in the convergent section and inlet total pressure on mass flow rate.

Condition	P_{0in} (kPa)	Q_c (J/mm s)	Mass flow rate (kg/s)	Mass flow rate reduction (%)	Increase in P_{0in} (%)
Adiabatic	142.4	0	0.6886	0	0
Case 1	142.4	340	0.6690	2.85	0
Case 2	146.3	340	0.6886	0	2.74

Table 2: Amount of inlet total pressure for fixing mass flow rate.

Condition	P_{0in} (kPa)	Q_c (J/mm s)	Mass flow rate (kg/s)	Increase in P_{0in} (%)
Adiabatic	142.4	0	0.6886	0.00
Heat case 1	143.7	112	0.6886	0.91
Heat case 2	145.0	225	0.6886	1.83
Heat case 3	146.3	340	0.6886	2.74
Heat case 4	147.2	419	0.6886	3.37

Figures 6 and 7 show the variations of degree of supercooling and the nucleation rate along the nozzle length. It is observed that the flow heating causes a delay in the maximum of these parameters. However, the limited increasing of the inlet stagnation pressure has little effect on these parameters.

Considering the effects of heating on nucleation, it is expected that due to the effects of heating, the wetness fraction along the nozzle length is decreased; this is confirmed in Figure 8. Like previous diagrams, increasing the inlet stagnation pressure has no undesirable influences on this parameter. Variations of pressure ratio and Mach number along the divergent section are shown in Figures 9 and 10. These diagrams show that heating causes some delay in the location of the condensation shock. Also, fixing the mass flow rate by increasing the inlet stagnation pressure does not have any important effects on the pressure and Mach number along the nozzle.

Considering all the results, it is concluded that increasing the inlet stagnation pressure for keeping the mass flow rate constant, does not have unwanted effects on the main flow parameters. Therefore, this idea can be used as an approach for fixing the mass flow rate in heated or non-adiabatic two-phase steam flows.

3.2. Part II

In the second part, adiabatic flow with $P_{0in} = 142.4$ kPa is influenced by four different cases of heating rate and increased inlet stagnation pressure. In all cases, the mass flow rate is the same as the adiabatic value. In other words, regularly, with an increase in heating rate, the inlet stagnation pressure is increased to fix the mass flow rate. Table 2 shows that increasing the inlet stagnation pressure can stabilize the mass flow.

For further clarification, the total amount of heating the convergent section and the total latent heat released due to condensation in each case is shown in Table 3.

It is to be reminded that $Q_{Case4} > Q_{Case3} > Q_{Case2} > Q_{Case1} > Q_{Adiabatic}$ and also $(P_{Inlet})_{Case4} > (P_{Inlet})_{Case3} > (P_{Inlet})_{Case2} > (P_{Inlet})_{Case1} > (P_{Inlet})_{Adiabatic}$.

Regarding the previous paper of the author in [6] and the first part of the results, it is known that heating the convergent section with fixed inlet stagnation pressure causes a decrease

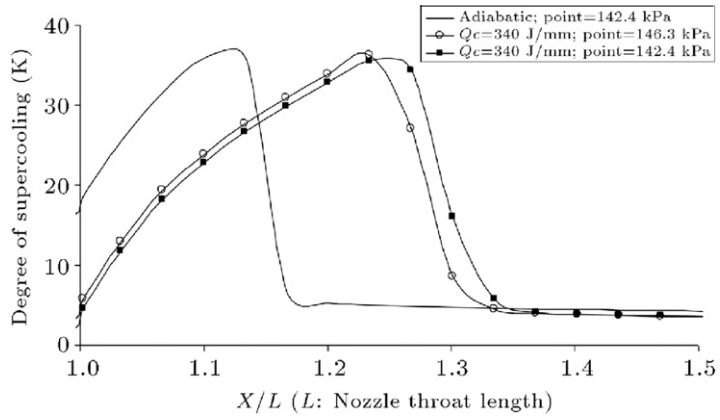

Figure 6: Variation of degree of supercooling in the divergent section (Part I).

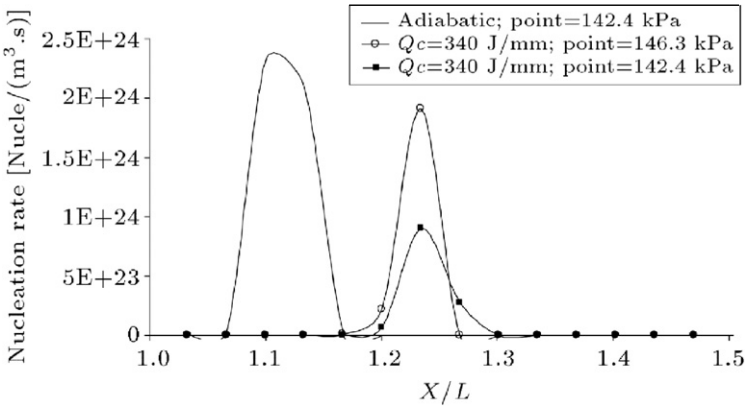

Figure 7: Variation of nucleation rate in the divergent section (Part I).

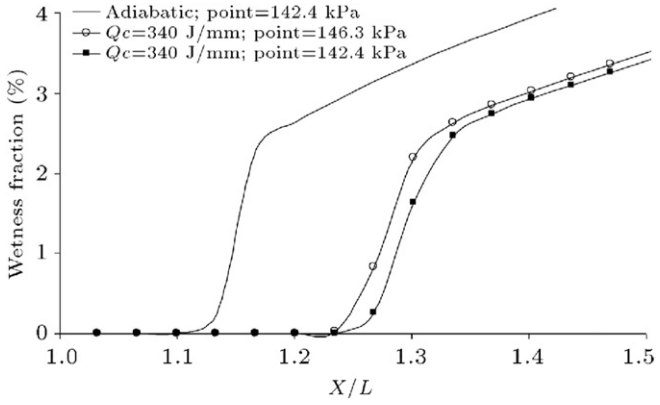

Figure 8: Variation of wetness fraction in divergent section (Part I).

Table 3: Total heat and total released latent heat in Part II.

	Total heat transfer to the convergent section (kJ/s)	Total released heat (kJ/s)
Adiabatic	0.00	116.12
Heat case 1	8.43	110.27
Heat case 2	17.00	104.25
Heat case 3	25.64	98.05
Heat case 4	31.66	96.04

in the super-saturation ratio and degree of supercooling, postpones their maximum and, finally, decreases the nucleation rate. On the other hand, heating the dry flow in the convergent section makes some limited mass flow rate reduction that can be recovered by slightly increasing the inlet stagnation pressure.

As expected, heating the dry flow in the convergent channel causes some delay in the maximum degree of supercooling and nucleation rate, as shown in Figures 11 and 12. Heating the dry steam flow in the convergent section and rising the inlet stagnation pressure have two opposite effects on the maximum degree of supercooling and nucleation rate. The first one increases the maximum value, while the second one decreases it. Therefore, the maximum amounts of these two

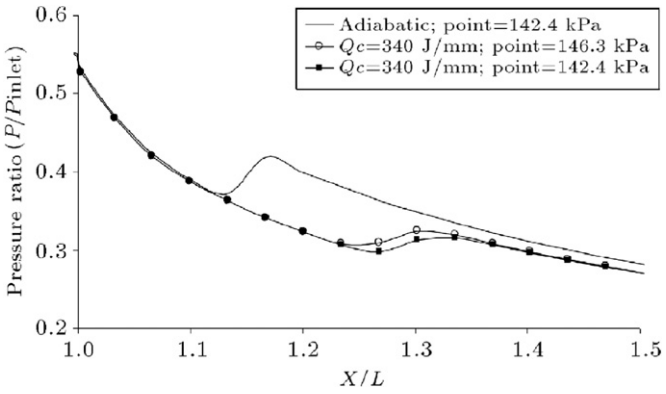

Figure 9: Variation of pressure ratio in the divergent section (Part I).

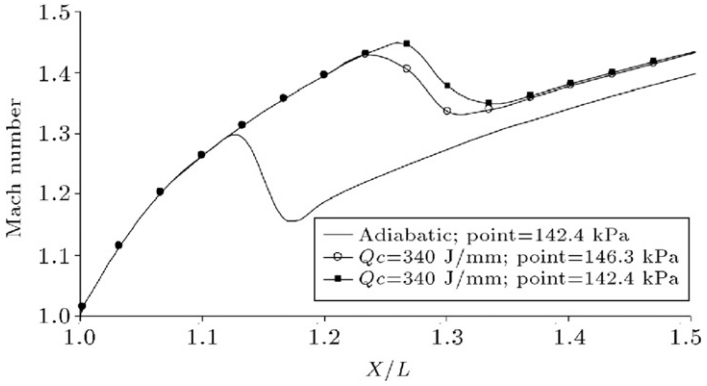

Figure 10: Variation of Mach number in the divergent section (Part I).

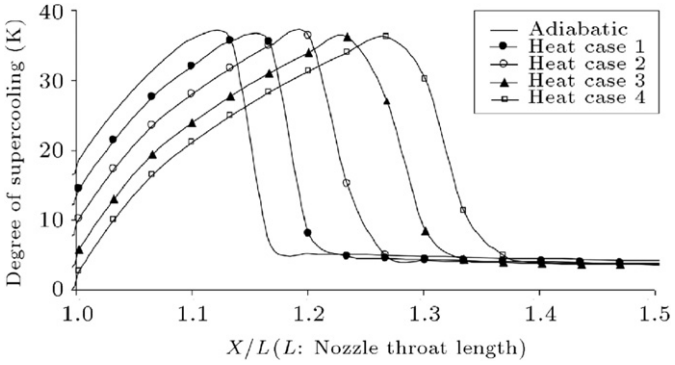

Figure 11: Variation of degree of supercooling in the divergent section (Part II).

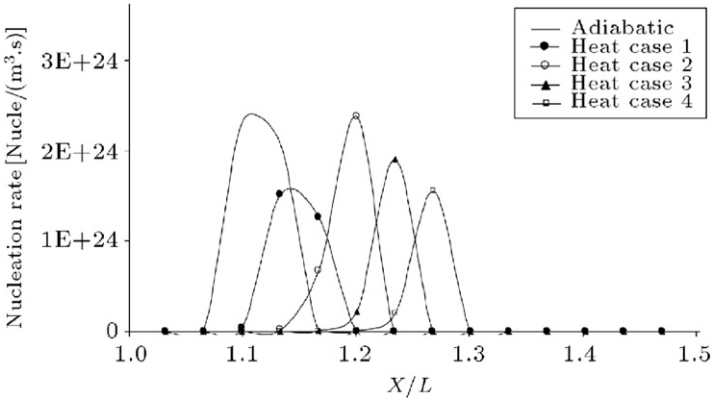

Figure 12: Variation of nucleation rate in the divergent section (Part II).

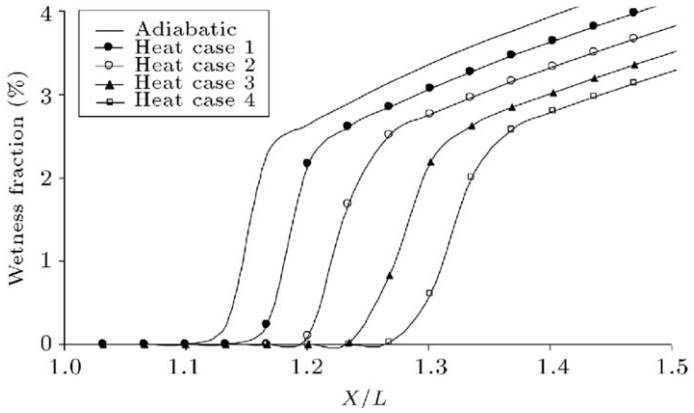

Figure 13: Variation of wetness fraction in the divergent section (Part II).

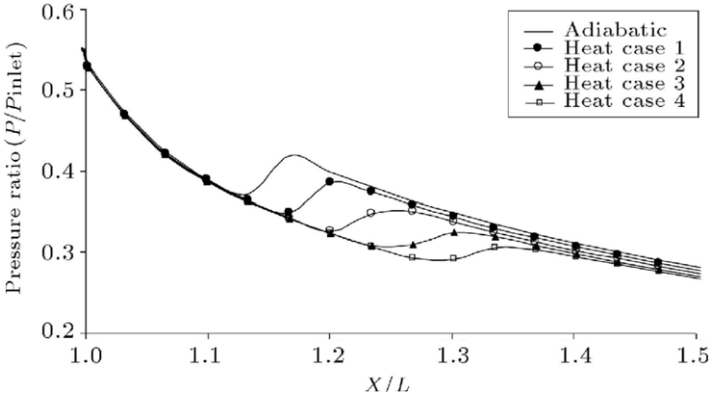

Figure 14: Variation of pressure ratio in the divergent section (Part II).

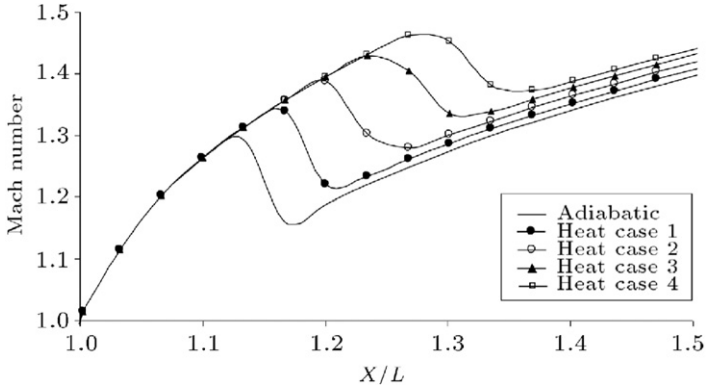

Figure 15: Variation of Mach number in the divergent section (Part II).

parameters depend on the interaction of these two opposite factors. In the first heating case, heating is the dominant factor and causes the maximums of these parameters to decrease. In heating case 2, rising stagnation pressure dominates and the maximum value is increased. In heating cases 3 and 4 the maximum degree of supercooling and nucleation rate decreases uniformly. It should also be noted that the differences between the maximum values in different cases are very small.

Considering the nucleation rate in Figure 12, it is expected that increasing the heating rate, and also the inlet stagnation pressure, lowers the wetness fraction, which is confirmed in Figure 13.

It is observed in Figure 14 that increasing the heating rate, and also raising the inlet stagnation pressure, relocates the condensation shock to the outlet of the nozzle, which is compatible with nucleation and wetness fraction diagrams.

In Figure 15, variations of the Mach number are shown and they are similar to pressure distributions in Figure 14, but, in the opposite trend. Figure 16 shows the variation of vapor temperature along the divergent section of the nozzle where the non-equilibrium steam flow starts nucleating and changing to the wet steam or equilibrium two-phase flow. Increase in the heating rate increases vapor temperature before the condensation shock, but, after that, considering the pressure ratio diagram and proportion between temperature and pressure, the temperatures are the same.

Figures 14–16 show that changes in the inlet stagnation pressure do not have significant effects on the condensation

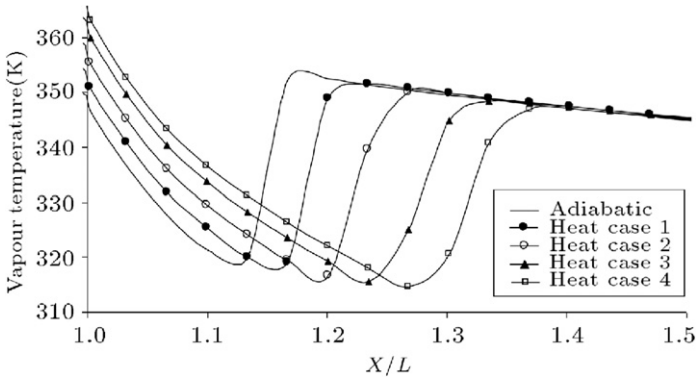

Figure 16: Variation of vapor temperature in the divergent section (Part II).

Table 4: Entropy generation in the divergent section for cases in Part II.

Condition	Entropy generation (J/kg K s)
Adiabatic	13.20
Heat case 1	13.70
Heat case 2	14.18
Heat case 3	14.13
Heat case 4	14.55

shock parameters, and the dominant factor is the heating rate to dry steam flow.

Similar to nucleation, increasing the heating rate and the inlet stagnation pressure has opposite effects on entropy generation. Increasing the heating rate decreases the nucleation rate and, therefore, lessens the entropy generation in the divergent section. However, increasing the inlet stagnation pressure increases the entropy generation; total entropy generation in the divergent section for different cases is shown in Table 4.

As shown in Table 4, increasing the inlet stagnation pressure is the dominant factor for the entropy generation.

4. Conclusions

Based on the presented diagrams and the results of the previous study by the authors [6], it is concluded that volumetric heating of the convergent section of a Laval nozzle can improve the wetness parameters and increase the efficiency and stability of the flow.

However, the investigations also reveal that these positive effects are accompanied by an undesirable side effect, i.e. the reduction of the mass flow rate up to 5%, which can decrease the output power of the steam turbine.

To solve this problem, it is suggested that based on the rate of volumetric heating to dry steam flow, the desired mass flow rate, and also assuming fixed inlet total temperature, the inlet stagnation pressure should be increased. Based on this approach, one adiabatic case and four different heat rates have been investigated. Investigating the results, it is inferred that by adjusting the inlet stagnation pressure in different heat rates, in addition to improving the wetness parameters and condensation shock effects, the mass flow rate of the nozzle is fixed, while having a limited increase in generated entropy. Therefore, it is concluded that by selecting a suitable volumetric heat rate and applying a proportionate increase to the inlet stagnation pressure, the efficiency and stability of the flow can be improved, while fixing the mass flow rate in comparison to the same conditions in an adiabatic case.

References

[1] Kulmala, M. "Condensational growth and evaporation in the transition regime", *Aerosol Scicncc and Technology*, 19, pp. 381–388 (1993).
[2] Bakhtar, F., Zamri, M.Y. and Rodriguez-Lelis, J.M. "A comparative study of treatment of two-dimensional two-phase flows of steam by a Runge–Kutta and by Denton's methods", *Proceedings of the Institution of Mechanical Engineers, Part C: Journal of Mechanical Engineering Science*, 221(C6), pp. 689–706 (2007).
[3] Mashmoushy, F., Mahpeykar, M.R. and Bakhtar, F. "Studies of nucleating and wet steam flows in two-dimensional cascades", *Journal of Mechanical Engineering Science IMechE*, 218(8), pp. 843–858. Part C (2004).
[4] Gerber, A.G. and Kermani, M.J. "A pressure based Eulerian–Lagrangian multi-phase model for non-equilibrium condensation in transonic steam flow", *International Journal of Heat and Mass Transfer*, 47(10–11), pp. 2217–2231 (2004).
[5] Sasao, Y. and Yamamoto, S. "Numerical prediction of humid effect to transonic flows in turbomachinery", *Proceedings of the International Gas Turbine Congress Tokyo* (2003).
[6] Mahpeykar, M.R., Teymourtash, A.R. and Amiri Rad, E. "Reducing entropy generation by volumetric heat transfer in a supersonic two-phase steam flow in a Laval nozzle", *International Journal of Exergy (IJEX)*, 9(1) (2011).
[7] Peeters, P., Luijten, C.C.M. and van Dongen, M.E.H. "Transitional droplet growth and diffusion coefficients", *International Journal of Heat and Mass Transfer*, 44(1), pp. 181–193 (2001).
[8] Cinar, G., Yilbas, B.S. and Sunar, M. "Study into nucleation of steam during expansion through a nozzle", *International Journal of Multiphase Flow*, 23(6), pp. 1171–1188 (1997).
[9] Kantrowitz, A. "Nucleation in very rapid vapour expansion", *Journal of Chemical Physics*, 19, p. 1097 (1951).
[10] Courtney, W.G. "Remarks on homogeneous nucleation", *Journal of Chemical Physics*, 35, p. 2249 (1961).
[11] Wolk, J., Strey, R., Heath, H.C. and Wialouzil, B.E. "Empirical function for homogeneous water nucleation rates", *Journal of Chemical Physics*, 117(10), pp. 4954–4960 (2002).
[12] Hale, B.N. and DiMattio, D.J. "Scaling of the nucleation rate and a Monte Carlo discrete sum approach to water cluster free energies of formation", *Journal of Physical Chemistry B*, 108, pp. 19780–19785 (2004).
[13] Hale, B. "Temperature dependence of homogeneous nucleation rates for water: near equivalence of the empirical fit of Wölk and Strey and the scaled nucleation model", *Journal of Chemical Physics*, 122, pp. 204509-1–204509-3 (2005).
[14] Sinha, S., Wyslouzil, B.E. and Wilemski, G. "Modeling of H2O/D2O condensation in supersonic nozzles", *Aerosol Science and Technology*, 43, pp. 9–24 (2009).
[15] Mahpeykar, M.R. and Amiri Rad, E. "The suppression of condensation shock in wet steam flow by injecting water droplets in different regions of a Laval nozzle", *Scientia Iranica, Transaction B*, 17(5), pp. 337–347 (2010).
[16] Senoo, S. and White, A.J. "Numerical simulation of unsteady wet steam flows with non-equilibrium condensation in the nozzle and the steam turbine", *ASME Joint US-European Fluid Engineering Summer Meeting* (2006).
[17] Hiwase, S.D., Datta, A. and Som, S.K. "Entropy balance and exergy analysis of the process of droplet combustion", *Journal of Physics D: Applied Physics*, 31(13), p. 1601 (1998).

Ehsan Amiri Rad received a B.S. degree in Mechanical Engineering from Iran University of Science and Technology in 2005, and an M.S. degree (in Energy Conversion) and a Ph.D. degree from Ferdowsi University of Mashhad, Iran, in 2007 and 2011, respectively. He has published more than six papers in journals and international conference proceedings. Currently he is Assistant Professor at Hakim Sabzevari University, Iran.

Mohammad Reza Mahpeykar has been a Professor of Mechanical Engineering at Ferdowsi University of Mashhad, Iran, since 1992. He received a B.S. degree in Mechanical Engineering from Ferdowsi University of Mashhad, Iran, in 1981, and an M.S. degree in Fluid Mechanics, and a Ph.D. degree in Energy Conversion from Birmingham University, UK, in 1987 and 1992, respectively. He has published more than seven books in Mechanics and Industrial Engineering and about 70 papers in respected journals and international conference proceedings. He is Chief Editor of the Journal of Applied Sciences and Computational Mechanics published by Ferdowsi University of Mashhad, Iran.

Ali Reza Teymourtash received a B.S. degree in Mechanical Engineering from Ferdowsi University of Mashhad, Iran, in 1983, an M.S. degree in Mechanical Engineering (Thermofluids) from Sharif University of Technology, Tehran, Iran, in 1987, and a Ph.D. degree in Energy Conversion from Ferdowsi University of Mashhad, Iran, in 2002, where he is now Associate Professor.

He has published a book in Fluid Mechanics, 25 papers in respected international conference proceedings and 19 journal papers. He has also been responsible for a number of applied industrial projects.